Vol. 4, No. 8 August 1994
GSA TODAY
A Publication of the Geological Society of America

INSIDE

Fractal Aspects of Geomorphic and Stratigraphic Processes

Donald L. Turcotte, Department of Geological Sciences, Cornell University, Ithaca, NY 14853

Erosional drainage pattern in the southern Basin and Range region, western United States (courtesy of Arthur Bloom, Cornell University).

ABSTRACT

Fractal behavior implies power-law, scale-invariant statistics; these statistics are applicable to a wide variety of geological problems. Although topography is often complex, statistically, it usually exhibits fractal behavior; drainage networks are a classic example of a fractal tree. High stands and low stands in reservoirs have been demonstrated to obey fractal, power law statistics; there is also evidence that peak river discharges during floods obey fractal statistics. Floods are responsible for the deposition of some sedimentary sequences; sedimentary layering under a variety of circumstances satisfies fractal statistics.

INTRODUCTION

The subjects of hydrology, geomorphology, sedimentology, and stratigraphy are interrelated. Landforms are created by tectonic processes but are destroyed by erosion; sediment erosion and deposition are primarily responsible for the surface morphology of the continents. Erosion is dominated by floods, but it is a subject of controversy whether erosion is dominated by the very largest floods or a characteristic flood, say the 10 year or 100 year flood. Erosional processes are responsible for the development of drainage networks, which in turn dominate the development and evolution of landforms. The deposition of sediments is responsible for the development of stratigraphic sequences. These sequences may contain a wealth of information on paleoweather and climate if they can be interpreted.

It is easy to argue that the coupled processes of rainfall, runoff, erosion, material transport, and deposition are so complex as to defy analysis. Yet it must be recognized that there is considerable order in this complexity; fractal statistics are widely applicable. Self-similar fractals are defined by the relation

$$N = C_1 r^{-D} \text{ or } D = \frac{\log (N_u/N_{n+1})}{\log (r_{n+1}/r_n)} \tag{1}$$

where D is the fractal dimension, N is the number of objects with a linear dimension r, and C is a constant of proportionality. The concept of fractals was introduced by Mandelbrot (1967) in terms of the length of the west coast of Great Britain. His result is given in Figure 1A; the measured length P of the coast line is given as a function of the length r of the measuring rod. Good agreement with the fractal relation

$$P = Nr = C_1 r^{1-D} \tag{2}$$

is found taking $D = 1.25$. Similar results are obtained for the length of contours on topographic maps; three examples are also given in Figure 1 for diverse geologic settings. It is seen that there is little variation in the fractal dimension (1.15–1.25); the fractal dimension of topography is not sensitive to the geologic setting and is not diagnostic of age.

The height of topography along a linear track is equivalent to a time series[1]. It is common practice to expand a time series in a Fourier series over the interval L; the coefficients in the Fourier series A_n correspond to the wave length $\lambda_n = 2\pi/k_n$, with k_n the wave number. The spectral power density of a time series is given by $S_n = A_n^2 L$. A time series is a self-affine fractal if (Turcotte, 1992)

$$S_n = C_2 k^{-\beta} \text{ or } A_n = C_3 \lambda_n^{\beta/2}. \tag{3}$$

The corresponding self-affine fractal dimension is given by $D = 1/2(5 - \beta)$.

Spherical harmonic expansions of the topography on a planet are equivalent to the Fourier expansion of a time series. Spherical harmonic expansions of the global topography of Earth (Rapp, 1989) and Venus are given in Figure 2. In both cases, good agreement with equation 3 is obtained taking $\beta = 2(D = 1.5)$; this is equivalent to the result $A_n = C_3 \lambda_n$. In the spectral domain, mountains have the same height to width ratios independent of size.

From Figure 2 it is seen that the amplitude of the topography on Venus, A_n, is about a factor of four less than on Earth; but on both planets the topography has the same spectral dependence $\beta = 2$. This is somewhat surprising because erosion is dominant in the evolution of many landforms on Earth; erosion is virtually absent on Venus, so that tectonic processes are dominant. This suggests that the tectonic processes that build topography and the erosional processes that destroy topography both give the same statistical behavior. Once again, the fractal dimension of topography does not appear to be diagnostic. It should also be pointed out that the fractal dimensions of topography associated with self-affine spectral expansions and self-similar coastline lengths are not, in general, equal. However, under a wide variety of conditions, topography does obey fractal statistics to a good approximation.

Drainage networks are classic examples of fractal trees. It is standard practice in geomorphology to use the Strahler (1957) ordering system. When two like-order streams meet, they form a stream with one higher order than the original. Thus, two first-order streams combine to form a second-order stream, two second-order streams combine to form a third-order stream, and so forth. The bifurcation ratio R_b is defined by

$$R_b = \frac{N_n}{N_{n+1}}, \tag{4}$$

where N_n is the number of streams of order n. The length-order ratio R_r is defined by

$$R_r = \frac{r_{n+1}}{r_n}, \tag{5}$$

where r_n is the mean length of streams of order n. From equation 1 the fractal dimension of a drainage network is (La Barbera and Rosso, 1989)

$$D = \frac{\ln R_b}{\ln R_r}. \tag{6}$$

Horton's (1945) laws require that R_b and R_r be nearly constant for a range of stream orders in a drainage basin; thus, drainage networks were recognized as

Fractal *continued on p. 211*

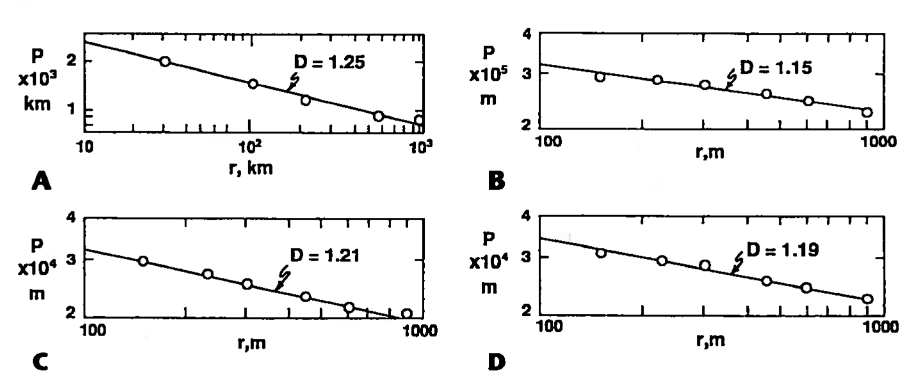

Figure 1. A: Length P of the west coast of Great Britain as a function of the length r of the measuring rod. B–D: Lengths P of specified topographic contours in several mountain belts as a function of the length r of the measuring rod; B: 3000 ft contour of the Cobblestone Mountain quadrangle, Transverse Ranges, California; C: 10,000 ft contour of the Byers Peak quadrangle, Rocky Mountains, Colorado; D: 1000 ft contour of the Silver Bay quadrangle, Adirondack Mountains, New York. Correlations are with the fractal relation shown in equation 2.

[1]*Editor's note:* For those readers who are, as I am, mathematically deprived, a Fourier series can be used to approximate a complex curve by addition of a number of sine and cosine waves of different wavelength (λ_n) and amplitude (A_n).
—*E. M. Moores*

Fractal *continued from p. 201*

being fractal 20 years before the concept of fractals was defined.

Important aspects of surface morphology obey fractal statistics; but the nagging question is, Why? Are the processes that create landforms scale invariant and the only scale-invariant statistics fractal? Or are the underlying processes in a class that generates fractal statistics?

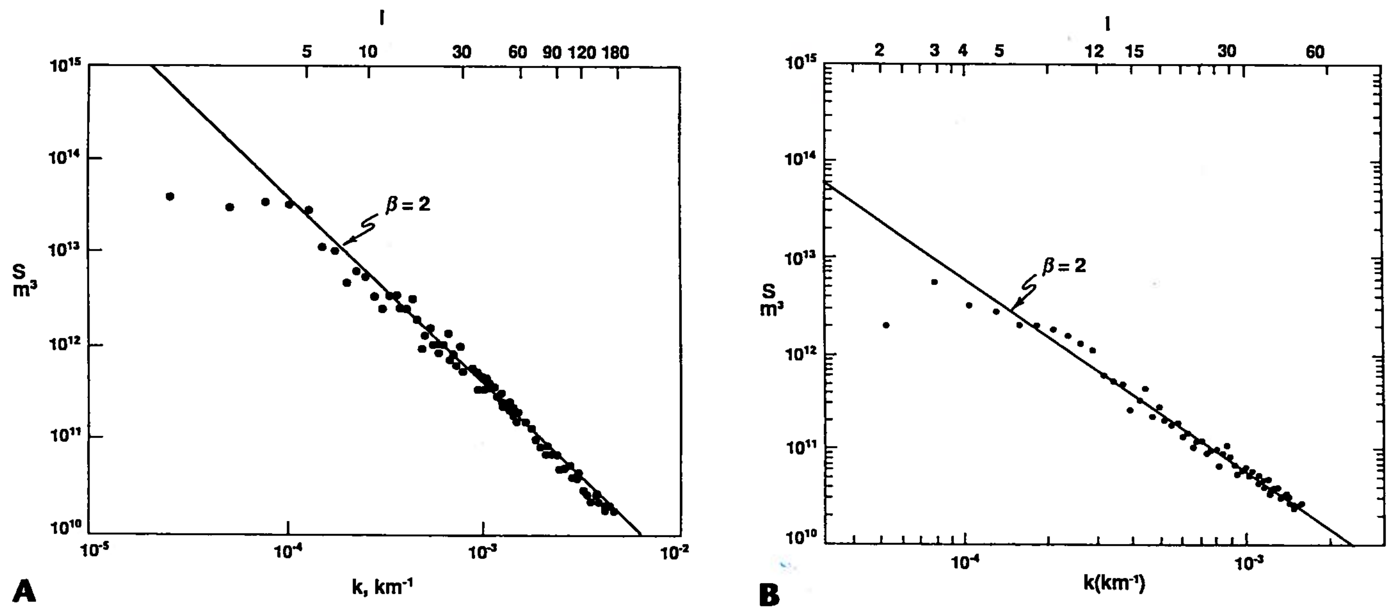

Figure 2. Power spectral density, S, as a function of wave number, k, for spherical harmonic expansions of topography (degree ℓ) for Earth (A) and Venus (B). Correlations are with equation 3, taking $\beta = 2$.

FLOOD STATISTICS

An important question in geomorphology concerns which floods dominate erosion. Is erosion dominated by the 10-year, the 100-year, or the very largest floods? The answer to this question depends upon whether extreme flood probabilities have a logarithmic or power-law dependence on time. The peak river discharge $\dot{V}$ during a flood is a measure of its intensity. If floods have a logarithmic dependence on time, the peak discharge $\dot{V}$ during the most severe flood in a time interval T depends on T according to

$$\dot{V} = C_4 \log T + C_5 . \qquad (7)$$

If floods have a power-law (fractal) dependence on the interval, then we have

$$\dot{V} = C_6 T^H . \qquad (8)$$

With the logarithmic dependence, extreme floods are much less likely to occur than with the power-law dependence. Thus, the more frequent, intermediate-size floods will carry the bulk of the eroded sediments rather than the rare extremely large flood. With a power-law dependence, the very largest floods are generally responsible for the bulk of sediment transport. Flood-frequency statistics also have a variety of other implications; land-use regulations and flood control projects are based on extrapolations for future floods.

Records of the peak flood discharges are generally available for a relatively short period of time; typically 50 to 100 years in the United States. The objective of flood-frequency analysis is to extrapolate the historical record to longer periods of time. A wide variety of statistical distributions have been utilized for this purpose; Turcotte and Greene (1993) have suggested the applicability of the fractal relation in equation 8. The fractal distribution can also be expressed in terms of the ratio F of the peak discharge over a 10-year interval to the peak discharge over a one-year interval. With self-similarity, the parameter F is then also the ratio of the 100-year peak discharge to the 10-year peak discharge and the 1000-year peak discharge to the 100-year peak discharge. The parameters H and F can be related by

$$F = 10^H . \qquad (9)$$

We refer to the parameter F as the flood intensity factor.

As two specific examples we consider station 1-1805 on the Middle Branch of the Westfield River in Goss Heights, Massachusetts, for the period 1911–1960 and station 11-0980 in the Arroyo Seco near Pasadena, California, for the period 1914–1965. These stations were chosen because they were two of the ten stations used as benchmarks by Benson (1968), who applied a variety of geostatistical distributions to flood-frequency forecasting. Floods are considered independent only if the peak flows are separated by more than one month. For a 50-year record, the 50 largest values of $\dot{V}_m$ are ordered, the largest $\dot{V}_m$ is assigned a period $T = 50$ yr, the second largest flood a period $T = 50/2 = 25$ yr, the third largest flood a period $T = 50/3 = 16.7$ yr, and so forth. The results for the two stations are given in Figure 3.

For station 1-1805 the fractal fit (F) gives $H = 0.51$ and $F = 3.3$. For station 11-0980 the fractal fit gives $H = 0.87$ and $F = 7.4$. Also included in Figure 3 are the six statistical correlations given by Benson (1968): the two-parameter gamma (Ga), Gumbel (Gu), log Gumbel (LGu), log normal (LN), Hazen (H), and log Pearson type III (LP). For large floods the fractal predictions (F) correlate best with the log Gumbel (LGu), while the other statistical techniques predict longer recurrence time for very serious floods. The fractal and log Gumbel are essentially power-law correlations, whereas the others are essentially logarithmic. The log Pearson type III (LP) is the federally approved distribution for evaluating the flood hazard in the United States. For station 1-1805 the 100 year flood predicted by the fractal correlation is a factor of 1.6 greater than the 100 year flood predicted by the log Pearson type III correlation. For station 11-0980 the 100 year flood predicted by the fractal correlation is a factor of 2.3 greater than the 100 year flood predicted by the log Pearson type III correlation. If, in fact, fractal statistics are applicable, then the use of log Pearson type III statistics consistently underestimates the severity of the 100, 150, and 200 year floods.

The values of H and the flood intensity factor F for the ten benchmark stations considered by Benson (1968) are given in Table 1. These results show that there are clear regional trends in the values of F. The values in the southwest are systematically high; this can be attributed to the arid conditions and the rare tropical storm that causes severe flooding. The values in the Pacific northwest are low; this can be attributed to the maritime climate. Because F is equivalent to a fractal dimension, $D = 2 - \log F$, this may be a case in which the fractal dimension of floods is diagnostic of climate.

The flow in a river is equivalent to a time series. The sum or integral of the flow in a river gives the volume of water stored in a reservoir. Harold Hurst spent his life studying reservoir storage on the Nile and concluded that extreme high stands and low stands in reservoirs obey power-law (fractal) statistics (Hurst et al., 1965). The relations between Hurst's work and self-affine fractals have been considered in detail by Mandelbrot and Wallis (1969a, 1969b).

DRAINAGE NETWORKS

Floods cause erosion, and this erosion eventually forms drainage networks. An example of a drainage network is given in Figure 4A; this is the drainage network in the Volfe and Bell Canyons, San Gabriel Mountains, near Glendora, California, obtained by field mapping (Maxwell, 1960). On average, one lower order of streams was found than on standard topographic maps; thus, the lowest order streams are assigned order 0. The number-length statistics for this network are given in Figure 5A; a good correlation with equation 6 was obtained taking $D = 1.81$. Leopold et al. (1964) have obtained similar results for the entire United States; a good correlation with equation 6 was also found with $D = 1.83$. Drainage networks are in general fractal, with little variation in the fractal dimension. Again, the fractal dimension of the drainage network is not diagnostic of its geologic setting.

Various statistical models were proposed in the 1960s in order to simulate drainage networks; this work was reviewed by Smart (1972). In the past

Fractal *continued on p. 212*

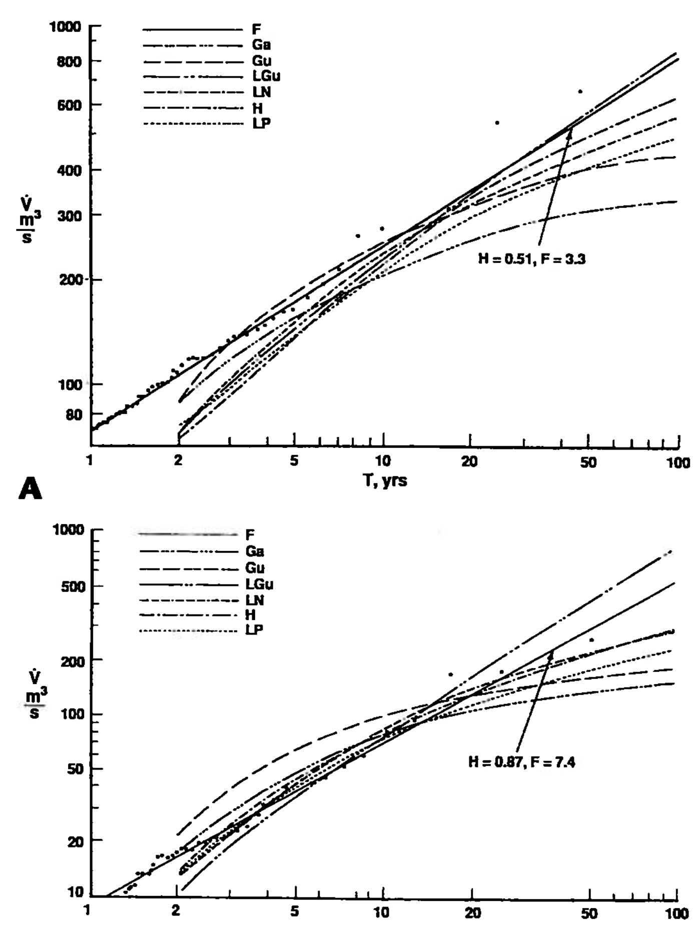

Figure 3. Peak discharge $\dot{V}$ during a flood associated with the period T. The dots are the sequence of observed floods. A: Middle Branch of the Westfield River at station 1-1805 in Goss Heights, Massachusetts. B: Arroyo Seco at station 11-0980 near Pasadena, California. Correlation lines are fractal (F), two parameter gamma (Ga), Gumbel (Gu), log Gumbel (LGu), log normal (LN), Hazen (H), and log Pearson type III (LP). The fractal correlations are with equation 8.

TABLE 1. VALUES OF H AND THE FLOOD INTENSITY FACTOR F FOR TEN BENCHMARK STATIONS

Station	Site	H	F
1-1805	Westfield River, Goss Heights, Mass.	0.513	3.31
2-2185	Oconee River, Greenboro, Ga.	0.540	3.47
5-3310	Mississippi River, St. Paul, Minn.	0.470	2.95
6-3440	Little Missouri River, Alzado, Wyo.	0.520	3.31
6-8005	Elkhorn River, Waterloo, Neb.	0.540	3.47
7-2165	Mora River, Golondinas, N. Mex.	0.630	4.27
8-1500	Llano River, Junction, Tex.	0.719	5.24
10-3275	Humboldt River, Comus, Nev.	0.616	4.13
11-0980	Arroyo Seco, Pasadena, Calif.	0.875	7.4
12-1570	Wenatchee River, Plain, Wash.	0.310	2.04

Note: Stations in Benson (1968) study.

Fractals *continued from p. 211*

three years there has been a rebirth of interest in the problem. Various models have been proposed by Willgoose et al. (1991), Meakin et al. (1991), Stark (1991), Chase (1992), Kramer and Marder (1992), and Inaoka and Takayasu (1993). As a typical example, we consider the diffusion-limited aggregation (DLA) model proposed by Masek and Turcotte (1993). We considered a square grid of points and introduced seed cells on the boundary of the grid. The mechanics of the model are illustrated in Figure 6. A square grid of 15 x 15 cells is used in this illustration. Five seed cells are introduced at random points on the lower boundary. The evolving network must grow from these seed cells. For the example shown, 16 cells have been accreted to the seed cells. Cells are allowed to accrete if one (and only one) of the four nearest neighbor cells is part of the preexisting network. Prohibited sites that already have two occupied neighboring sites are identified by stars. Sites available for accretion to the network are indicated by open circles. A random walker is introduced at a random cell on the grid, and the hypothetical path is traced by the solid line. After 28 random walks it accretes to the network at the shaded cell. A random walker proceeds until the walker either (1) accretes to the network, (2) exits the grid, or (3) lands on a prohibited cell. In each case the walk is terminated, and a new walker is introduced on a new, randomly selected site. The iteration of this basic procedure results in a branching network composed of linked drainage cells. A simulation carried out on a 256 x 256 grid is illustrated in Figure 4B; 20,000 random walkers have been introduced. The simulated and actual drainage networks are reasonably similar. The number-length statistics for the simulated network are given in Figure 5B; a good correlation with equation 6 is obtained taking D = 1.85. Again, good agreement is obtained between the simulated and real networks.

The random walkers can be interpreted as floods that flow over a relatively flat surface until they find a gully. When the flood enters the gully, it further erodes the gully and extends the network headward. This type of headward gully evolution has often been proposed for actual drainage networks (Schumm et al., 1987). The DLA model can also be used to generate synthetic topography. A power-law relation is assumed between stream order and gradient; the resulting topography is given in Figure 7.

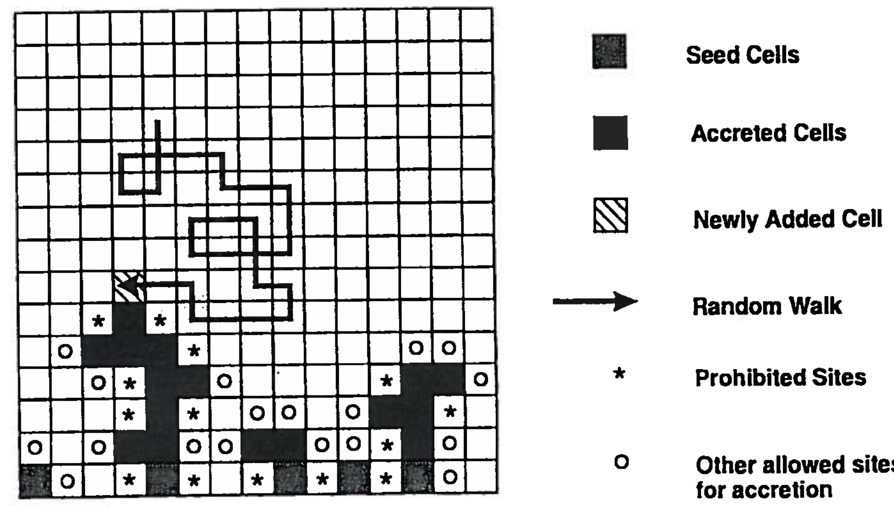

Figure 6. Illustration of the mechanism for network growth in the diffusion-limited aggregation (DLA) model. A random walker is randomly introduced to an unoccupied cell. The random walk proceeds until a cell is encountered with one (and only one) of the four nearest neighbors occupied (striped cell). The new cell is accreted to the drainage network; other allowed and prohibited sites are shown.

STATISTICS OF SEDIMENTARY LAYERS

Eroded sediments are eventually deposited as part of a layered sedimentary sequence. Each layer represents a distinct sedimentation event with an upward gradation from coarse-grained sediments to fine-grained sediments; individual layers are generally separated by well-defined bedding planes. Sediment deposition is a very complex series of processes. In some settings sediments are deposited directly by floods, as in deep lakes. In these cases it may be possible to infer flood-frequency statistics and paleoclimate from sedimentary layering statistics. Sediments deposited in shallow water can be transported and redeposited by storms. Despite the complexities, sediment layering under a variety of circumstances exhibits fractal statistics.

Two recent studies of the thickness statistics of turbidite deposits show fractal statistics. Rothman et al. (1994) carried out direct measurements on an outcrop of the Kingston Peak Formation near the southern end of Death Valley, California. Their results are given in Figure 8A; an excellent correlation with equation 1 is obtained taking D = 1.39. Hiscott et al. (1992) have studied a volcaniclastic turbidity-current deposit in the Izu-Bonin fore-arc basin offshore of Japan. Layer thicknesses were obtained from formation-microscanner images in the middle upper Oligocene part of the section. Results for two DSDP holes located 75 km apart are given in Figure 8B; a good correlation with equation 1 is obtained taking D = 1.12.

Turbidite deposits are associated with slumps off the continental margin. Although it is doubtful that the turbidite layer thicknesses scale directly with the sizes of slumps, it is likely that the fractal distribution of layer thicknesses implies a fractal size distribution of slumps. It is interesting to note that Bak et al. (1988) introduced the concept of self-organized criticality in terms of the size distribution of sand slides off sand piles. A conclusion of their studies was that the size distribution of sand slides should be fractal. Over the past several years, several laboratory studies have been carried out to determine the circumstances under which sand slides exhibit fractal statistics; this work was reviewed by Nagel (1992). The fractal statistics of turbidite layering is evidence that the associated slumping may be an example of self-organized criticality.

Fractal correlations of sedimentary sequences are not restricted to turbidite deposits. Stolum (1991) obtained fractal statistics for the Middle Jurassic Tiljo Formation in the North Sea Halten Bank basin; these sediments were deposited in a marine shelf environment. Stolum found values of D = 0.71, 0.80. Malamud and Turcotte (1992) obtained fractal statistics for sandy-bed thicknesses in the shallow marine environment of the Late Devonian Ithaca Formation, New York, with D = 1.41.

The fractal behavior of stratigraphic sequences has also been demonstrated using spectral techniques. Hewett (1986) gave results for a density-porosity log in a well through a late Miocene–early Pleistocene sandstone formation deposited in a deep submarine fan. He showed that the spectrum of the well log correlated with equation 3, taking β = 0.71. Similar results have been reported by Todoeschuck and Jensen (1988) and by Todoeschuck et al. (1990).

Hewett (1986) also developed a fractal-based interpolation technique for determining the porosity distribution in reservoirs. The three-dimen-

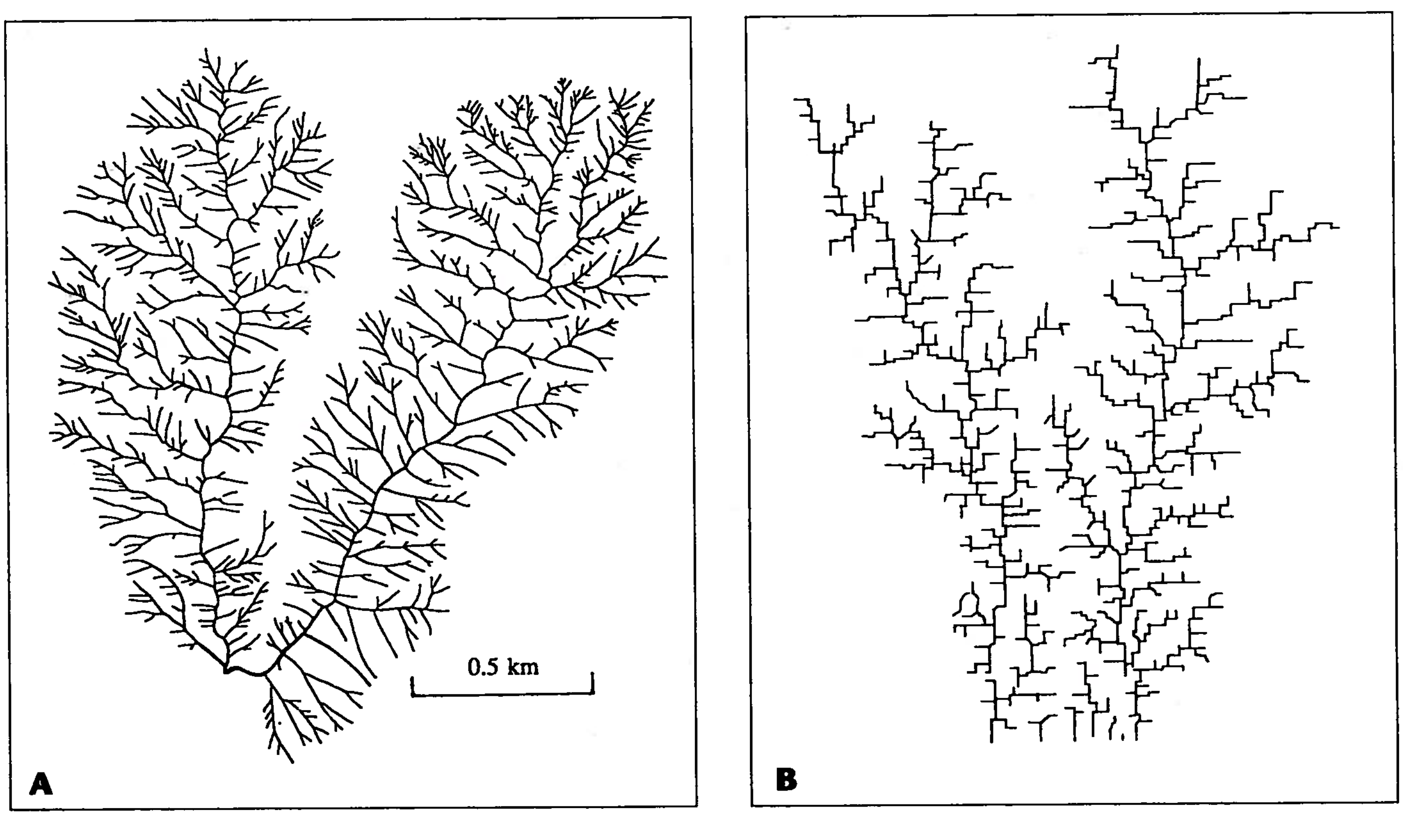

Figure 4. A: The drainage network in the Volfe and Bell Canyons, San Gabriel Mountains, near Glendora, California, obtained from field mapping. B: Illustration of a DLA model for a drainage network.

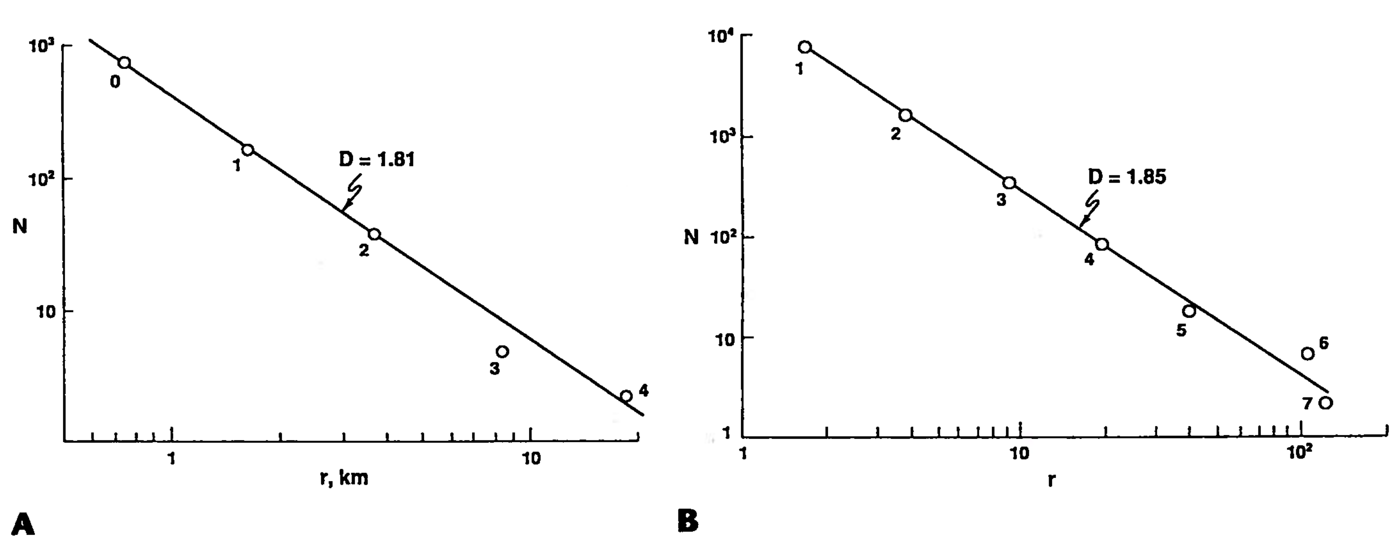

Figure 5. Dependence of the number of streams of various orders on their mean length for (A) the example illustrated in Figure 4A and (B) the model illustrated in Figure 4B. Each circle corresponds to the stream order indicated and the correlations are with equation 6.

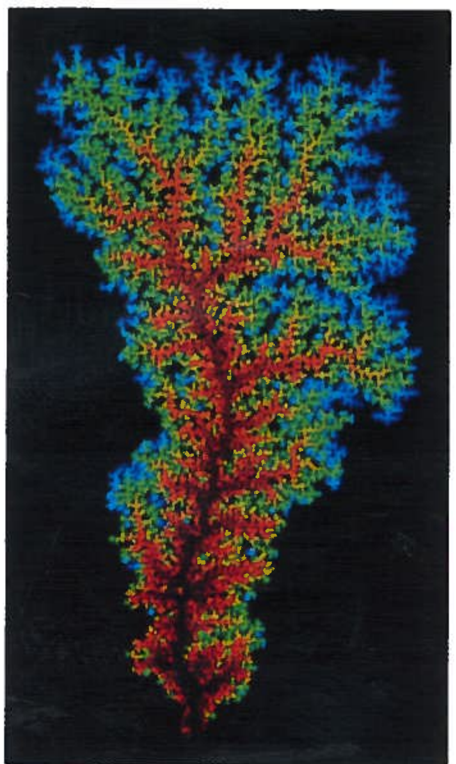

Figure 7. Color-coded topography generated by the DLA model.

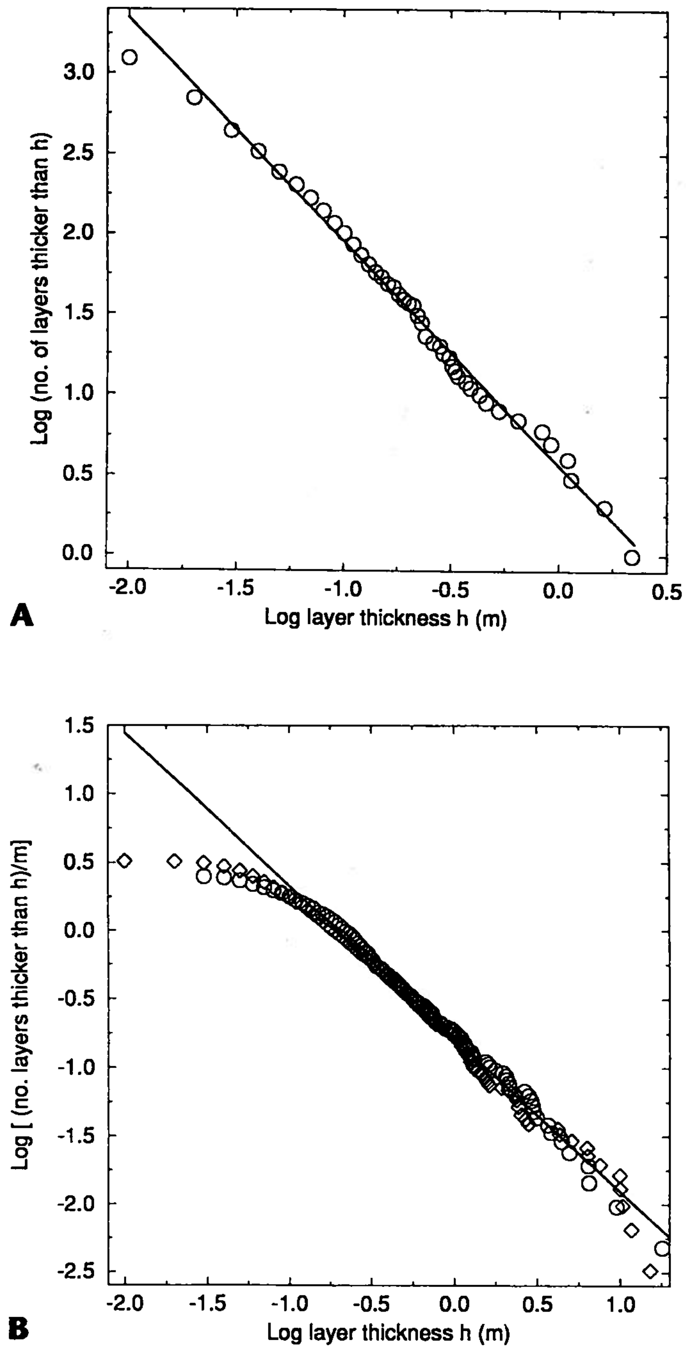

Figure 8. Frequency-thickness statistics for turbidite sequences of sedimentary layers. A: Kingston Peak Formation near the southern end of Death Valley, California. The total number of layers thicker than *h* is given as a function of *h*. B: Izu-Bonin fore-arc basin offshore of Japan. The circles are from Deep Sea Drilling Project (DSDP) hole 792 and the diamonds from DSDP hole 793. The number of layers per meter thicker than *h* is given as a function of *h*. Correlations with equation 1 yield D = 1.39 in A and D = 1.12 in B.

sional porosity of the reservoir was determined from a three-dimensional Fourier expansion. The coefficients in the vertical expansion were obtained from well logs. The coefficients in the horizontal expansions were scaled as the typical noise spectra of topography. The phases in the expansions were determined from well data. A synthetic example is given in Figure 9. This was obtained on a 256 x 256 grid, and the magnitude of the synthetic porosity in this cross section is arbitrary. The coefficients in the vertical Fourier expansion satisfied the fractal relation 3 with $\beta_y = 1.2$, and the coefficients in the horizontal Fourier expansions satisfied relation 3 with $\beta_x = 2.2$; the ratio of the vertical to horizontal coefficients was taken to be 5. With the ratios of the amplitudes of all coefficients determined by the fractal scaling, only the phases remain to be determined by the available data. Well-log data have been used, and the resulting fractal interpolations have been shown to be quite accurate in oil-field secondary recovery tests (Hewett, 1986).

DISCUSSION

Fundamental geomorphic and stratigraphic processes are relatively poorly understood. Some might say that the underlying processes of flooding, erosion, sediment transport, and stratigraphy are so complex as to defy successful modeling. Yet it is recognized that these processes satisfy fractal statistics under a wide variety of circumstances. There is a strong suggestion that modern approaches in statistical physics may be applicable to this class of problems. Examples include diffusion-limited aggregation and self-organized criticality; these approaches yield fractal statistics. In the past, these problems were commonly addressed by geostatistical empiricism. Flood-frequency analysis is an example. It will be exciting to see whether some or all of these processes can be modeled by the new approaches.

In addition, there is the suggestion that stratigraphic layering may contain a wealth of unused information. If the fractal dimension of floods is climate dependent and if stratigraphic sequences can be correlated directly with floods, then the sequences may provide improved data for the evaluation of the flood hazard today as well as providing a new database for paleoclimatology.

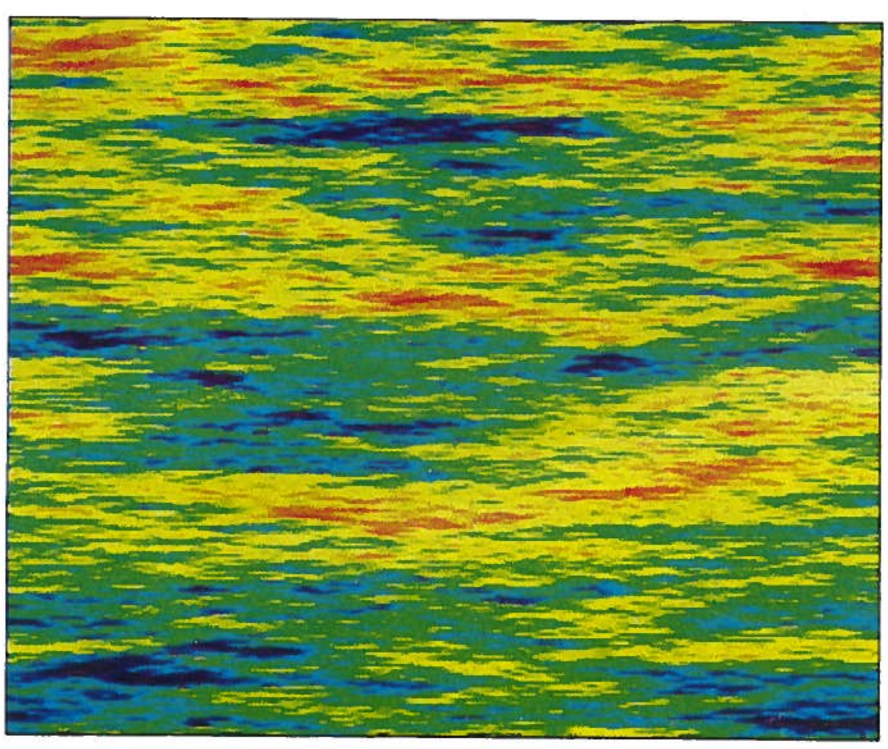

Figure 9. Cross section of a synthetic sedimentary sequence showing color-coded porosity. This is a self-affine fractal; it can be applied at any scale, but the vertical scaling is different from the horizontal scaling.

ACKNOWLEDGMENTS

The work on fractal flood frequency analysis was carried out by Lesley Greene and Kirk Haselton. The DLA model for drainage network illustrated in Figures 4, 5, 6, and 7 was developed by Jeff Masek. The synthetic fractal sedimentary cross section illustrated in Figure 9 was generated by Jie Huang. Bruce Malamud obtained thickness statistics on layered sedimentary cores.

REFERENCES CITED

Bak, P., Tang, C., and Wiesenfeld, K., 1988, Self-organized criticality: Physical Review, v. A38, p. 364–374.

Benson, M. A., 1968, Uniform flood-frequency estimating methods for federal agencies: Water Resources Research, v. 4, p. 891–908.

Chase, C. G., 1992, Fluvial landsculpting and the fractal dimension of topography: Geomorphology, v. 5, p. 39–57.

Hewett, T. A., 1986, Fractal distributions of reservoir heterogeneity and their influence on fluid transport: Society of Petroleum Engineers Paper 15386, 16 p.

Hiscott, R. N., Colella, A., Pezard, P., Lovell, M. A., and Malinverno, A., 1992, Sedimentology of deep-water volcaniclastics, Oligocene Izu-Bonin forearc basin, based on formation microscanner images, *in* Proceedings of the Ocean Drilling Program, Scientific results, Volume 126: College Station, Texas, p. 75–96.

Horton, R. E., 1945, Erosional development of streams and their drainage basins; hydrophysical approach to quantitative morphology: Geological Society of America Bulletin, v. 56, p. 275–370.

Hurst, H. E., Black, R. P., and Simaika, Y. M., 1965, Long-term storage: London, Constable, 145 p.

Inaoka, H., and Takayasu, H., 1993, Water erosion as a fractal growth process: Physical Review, v. E47, p. 899–910.

Kramer, S., and Marder, M., 1992, Evolution of river networks: Physical Review Letters, v. 68, p. 205–208.

La Barbera, P., and Rosso, R., 1989, On the fractal dimension of stream networks: Water Resources Research, v. 25, p. 735–741.

Leopold, L. B., Wolman, M. G., and Mille, J. P., 1964, Fluvial processes in geomorphology: San Francisco, W. H. Freeman, 522 p.

Malamud, B. D., and Turcotte, D. L., 1992, Frequency-size distributions of sandy-bed thicknesses in the shallow marine environment of the Late Devonian Ithaca Formation, New York State: Geological Society of America Abstracts with Programs, v. 24, no. 7, p. A357.

Mandelbrot, B. B., 1967, How long is the coast of Britain? Statistical self-similarity and fractional dimension: Science, v. 156, p. 636–638.

Mandelbrot, B. B., and Wallis, J. R., 1969a, Computer experiments with fractional Gaussian noises, Parts I, II, III: Water Resources Research, v. 5, p. 228–267.

Mandelbrot, B. B., and Wallis, J. R., 1969b, Robustness of the rescaled range R/S in the measurement of noncyclic long run statistical dependence: Water Resources Research, v. 5, p. 967–988.

Masek, J. G., and Turcotte, D. L., 1993, A diffusion-limited aggregation model for the evolution of drainage networks: Earth and Planetary Science Letters, v. 119, p. 379–386.

Maxwell, J. C., 1960, Quantitative geomorphology of the San Dimas experimental forest, California: Columbia University, Department of Geology Project NR 389-042, Technical Report 19.

Meakin, P., Feder, J., and Jossang, T., 1991, Simple statistical models for river networks: Physica, v. A176, p. 409–429.

Nagel, S. R., 1992, Instabilities in a sandpile: Reviews of Modern Physics, v. 64, p. 321–325.

Rapp, R. H., 1989, The decay of the spectrum of the gravitational potential and the topography of the Earth: Geophysical Journal International, v. 99, p. 449–455.

Rothman, D. H., Grotzinger, J., and Flemings, P., 1994, Scaling in turbidite deposition: Journal of Sedimentary Petrology, v. A64, p. 59–67.

Schumm, S. A., Mosley, M. P., and Weaver, W. E., 1987, Experimental fluvial geomorphology: New York, John Wiley, 413 p.

Smart, J. S., 1972, Channel networks: Advances in Hydroscience, v. 8, p. 305–346.

Stark, C., 1991, An invasion percolation model of drainage network evolution: Nature, v. 352, p. 423–425.

Stolum, H. H., 1991, Fractal heterogeneity of clastic reservoirs, *in* Lake, L. W., ed., Reservoir characterization II: San Diego, California, Academic Press, p. 579–612.

Strahler, A. N., 1957, Quantitative analysis of watershed geomorphology: Transactions, American Geophysical Union, v. 38, p. 913–920.

Todoeschuck, J. P., Jensen, O. G., 1988, Joseph geology and seismic deconvolution: Geophysics, v. 53, p. 1410–1414.

Todoeschuck, J. P., and Jensen, O. G., and Labonte, S., 1990, Gaussian scaling noise model of seismic reflection sequences: Evidence from well logs: Geophysics, v. 55, p. 480–484.

Turcotte, D. L., 1992, Fractals and chaos in geology and geophysics: Cambridge, U.K., Cambridge University Press, 221 p.

Turcotte, D. L., and Greene, L., 1993, A scale-invariant approach to flood frequency analysis: Stochastic Hydrology and Hydraulics, v. 7, p. 33–40.

Willgoose, G., Bras, R. L., and Rodriguez-Iturbe, I., 1991, A coupled channel network growth and hillslope evolution model, 1, Theory: Water Resources Research, v. 27, p. 1671–1684.

Manuscript received July 27, 1993; revision received January 7, 1994; accepted January 10, 1994 ■